

Article

Desulfurization of the Old Tailings at the Au-Ag-Cu Tiouit Mine (Anti-Atlas Morocco)

Abdelkrim Nadeif ¹, Yassine Taha ^{2,*} , Hassan Bouzahzah ³, Rachid Hakkou ^{1,2,*} and Mostafa Benzaazoua ^{4,5} 

¹ LCME, Faculté des Sciences et Techniques, Université Cadi Ayyad, Marrakech 40000, Morocco

² Materials Science and Nano-engineering Department, Mohammed VI Polytechnic University, Ben Guerir 43150, Morocco

³ GeMMe Laboratory, Argenco Department, Université de Liège, 4000 Liège, Belgium

⁴ Institut de Recherche en Mines et en Environnement, Université du Québec en Abitibi Témiscamingue, Rouyn-Noranda, QC J9X 5E4, Canada

⁵ Geology and Sustainable Mining Department, Mohammed VI Polytechnic University, Ben Guerir 43150, Morocco

* Correspondence: yassine.taha@um6p.ma (Y.T.); r.hakkou@uca.ma (R.H.)

Received: 30 April 2019; Accepted: 26 June 2019; Published: 30 June 2019



Abstract: Tailings from the abandoned Tiouit mine site in Morocco are mainly composed of sulfides, hematite, and quartz. They contain 0.06–1.50 wt % sulfur, mostly in the form of pyrite, pyrrhotite, and chalcopyrite. The tailings also contain gold (3.36–5.00 ppm), silver (24–37 ppm), and copper (0.06–0.08 wt %). Flotation tests were conducted to reprocess the tailings for Au, Ag, and Cu recovery, and at the same time to prevent acid mine drainage (AMD) generation through the oxidation of sulfide minerals, including pyrite, sphalerite, arsenopyrite, chalcopyrite, galena. The flotation results confirmed that environmental desulfurization is effective at reducing the overall sulfide content in the tailings. The recovery of sulfides was between 69% and 75%, while Au recovery weight-yield was between 2.8% and 4.7%. The test that showed the best sulfur recovery rate and weight-yield was carried out with 100 g/t CuSO₄ (sulfide activator) and 50 g/t of amyl xanthate (collector). The goal of this study was also to assess the remaining acid-generating potential (AP) and acid-neutralizing potential (NP) of the desulfurized tailing. The geochemical behavior of the initial tailings sample was compared to that of the desulfurized tailings using kinetic weathering cell tests. The leachates from the desulfurized tailings showed higher pH values than those from the initial tailings, which were clearly acid-generating. The residual acidity produced by the desulfurized tailings was most likely caused by the hydrolysis of Fe-oxyhydroxides.

Keywords: acid mine drainage; mine tailings; sulfides; gold reprocessing; desulfurization; flotation; kinetic test

1. Introduction

Acid mine drainage (AMD) generated by mine wastes and the subsequent contamination of surface waters and soils through leached metals is one of the most significant environmental problems facing the mining industry [1,2]. Higher operating costs result when AMD needs to be treated [3], and acid-generating wastes need to be reclaimed [4]. AMD is produced as a result of abiotic and biotic reactions involving water, air, and the sulfide minerals present in mine wastes (e.g., pyrite, pyrrhotite) [1,5,6]. These reactions produce acidic effluents that tend to be loaded with various heavy metals and metalloids (e.g., Fe, Mn, Cu, As, Hg) [1,2,7].

The need to manage sulfidic waste rocks and tailings is becoming an increasingly urgent issue. Safety issues (e.g., tailings dam failures), air pollution (e.g., dust generation), and water contamination (e.g.,

mine drainage) constitute the main concerns [8–10]. Many researchers have worked on the development of sustainable and eco-friendly solutions to eliminate or minimize the risks related to the disposal of mine tailings. Current waste management methods are site-specific and depend on local conditions. Tailings are generally stored in engineered dams and impoundments, dewatered, dried, and/or surface landfilled, stabilized with binders for open-pit or underground backfilling purposes [11,12]. Many challenges are faced such as seismicity risks, rainfall potential, land availability, etc.

Due to the depletion of metals ores and as these tailings could contain some valuable minerals, many studies were employed to investigate alternative technologies for a sustainable and integrated tailings management. Froth flotation has previously been used to recover Cu, Co, and other metals from tailings [13,14]. Prior works investigated the particle size of the tailings, the behavior of the froth during flotation, the age of the tailings, and the nature of the metal-bearing minerals (e.g., sulfides, oxides) as the main parameters affecting metal recovery [15–18]. Several recent studies also investigated bioleaching as a potential technology for removing heavy metals and sulfides from mine tailings [19–21]. Other innovative technologies for metal extraction from mine tailings were developed [22,23]. In addition to the reprocessing of mine tailings, researchers have also developed techniques for recycling mine tailings. For example, tailings could be put to use in products such as ceramics [24,25], and construction and building materials [26,27] among other applications [28].

Environmental desulfurization of tailings is one technology that has gained popularity in the last two decades. This method consists of separating sulfide minerals from mine tailings using froth flotation. The resulting desulfurized fraction can be managed separately [29,30] or backfilled in underground mines [31]. Desulfurization has been demonstrated as an economically and environmentally effective technique to decrease the acid-generation potential of mine tailings, in particular for operating mines and new mine projects [32–34].

Several old mine sites in Morocco have been abandoned without the implementation of proper closure plans, and most could still cause serious environmental damage [35]. The Tiouit Mine, which is located in the eastern Anti-Atlas Mountains, is one of these abandoned sites. From 1950 to 1996, the mine's Au, Ag, and Cu ore was estimated at approximately 1,743,000 tons [36,37]. Gold mineralization occurs exclusively as electrum as microscopic grains within various mineral phases. The gangue minerals consist of quartz, chlorite, and various feldspars. Approximately 743,000 tons of tailings were generated by the end of the mine's life and were landfilled in three tailings dams around the site [38]. The tailings facilities were abandoned without any restoration plans. The mine tailings contain 0.06–1.50 wt % sulfur, mostly in the sulfide minerals pyrite, pyrrhotite, and chalcopyrite [38]. AMD produced from these tailings has never been treated, resulting in the contamination of both surface and subsurface waters as well as the severe degradation of the surrounding ecosystems.

The main objective of this study was to investigate the feasibility of environmental desulfurization as a technique for reducing the acid-generating potential of the Tiouit mine tailings, while also recovering residual Au. The tailings samples were characterized for their main chemical and physical characteristics, as well as their acid-generating potential. A number of laboratory-scale flotation tests were conducted, using Denver flotation cells, to investigate precious metal recovery. Additionally, kinetic tests were performed to study the geochemical behavior of the desulfurized tailings, and consequently, determine the efficiency of the desulfurization process.

2. Materials and Methods

2.1. Tiouit Mine Site Description

Tiouit mine, discovered in 1947, is located in the eastern part of Jebel Saghro in the Anti-Atlas Mountains, Morocco, about 40 km south east of the city of Boumalne Dades. The Tiouit deposits were exploited intermittently by different companies: “Comansour” (1950–1956), “Westfield” (1959–1964), and finally the “SODECAT company” (1975–1996) [36]. The mineralization was identified as intrusive granite consisting of native gold associated with chalcopyrite (CuFeS_2), pyrite (FeS_2), sphalerite (ZnS),

galena (PbS), magnetite (Fe_3O_4), arsenopyrite (FeAsS), bornite (Cu_5FeS_4), luzonite (Cu_3AsS_4), gold (Au), and gray copper ($\text{X}_{12}\text{Y}_4\text{S}_{13}$, with X: Ag, Cu, Fe, Hg, Zn and Y: As, Sb, Te). The ore processing involved crushing and milling followed by a bulk froth flotation process [37,39,40]. Over the duration of the entire mining operation, more than 740,000 tons of mine tailings (168,000 tons in the northern tailings pond, 346,000 tons in the central tailings pond, and 229,000 tons in the southern tailings pond) were deposited at the surface without any reclamation measures (Figure 1). Larger volumes of mine wastes were discharged directly into the Tiout river. Many rainwater ravines were created in the tailings deposit, which caused their dispersion along the Tiout river.

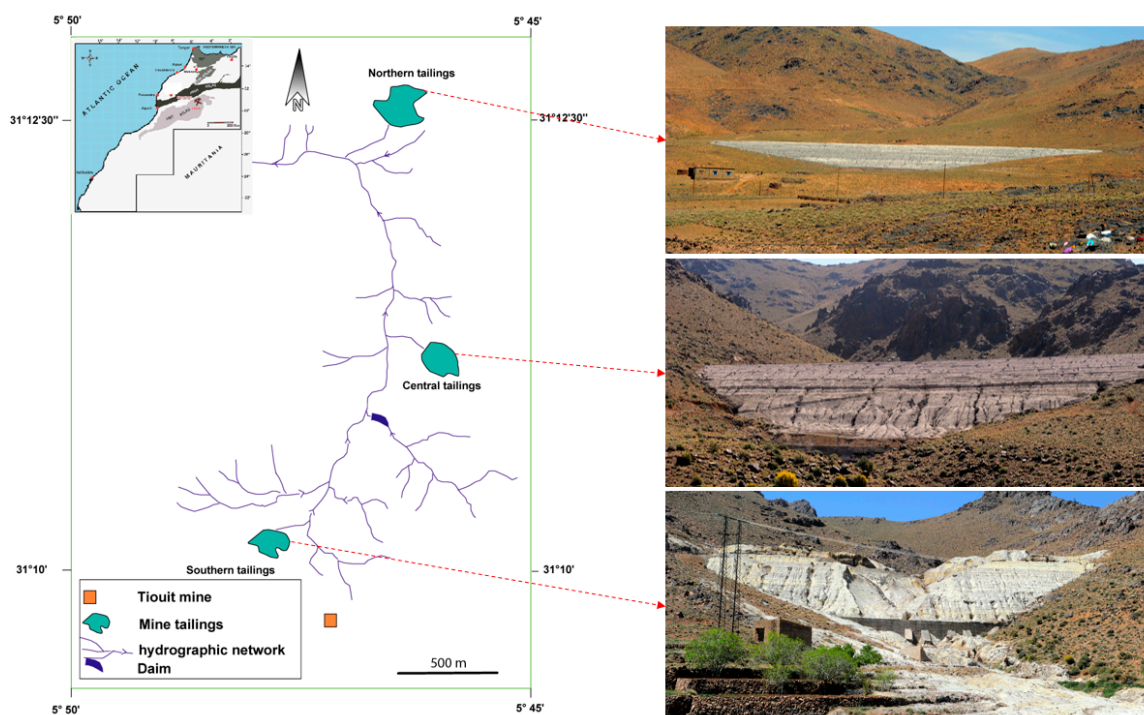


Figure 1. Tiout mine site location and photographs of northern, central, and southern tailing ponds.

2.2. Methodology

Tailings samples were collected after excavating trenches in the tailings ponds. Sampling sites were selected, based on field observations, to obtain fresh, non-oxidized tailings. Tailings samples labeled ST, CT, and NT were collected from the southern, central, and northern tailings ponds, respectively. Samples were collected at depths between 90 and 110 cm. All samples were carefully conditioned, and immediately stored in double-sealed plastic bags from which the air was evacuated to prevent contact with oxygen. A small, representative sample from each pond was stored at low temperature (5 °C) and at their original saturation (without drying) for kinetic testing. The methodology followed in this study is compiled in Figure 2. The aim was to desulfurize the sampled tailings to reduce their environmental impact. The floated sulfide-rich tailings (SRT) needed to be properly managed due to their high concentration of sulfides.

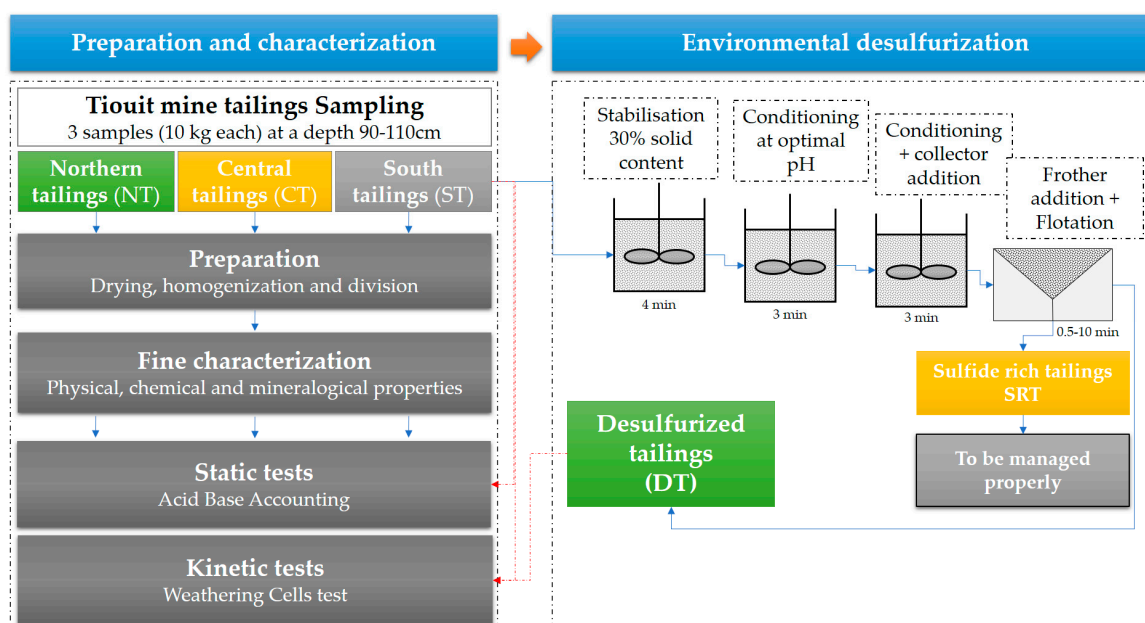


Figure 2. Schematic illustration of the methodology followed in this study.

2.2.1. Analytical Methods

Chemical compositions of the tailings samples were obtained by inductively coupled plasma atomic emission spectroscopy (ICP-AES; Perkin Elmer Optima 3100 RL, Waltham, MA, USA) following digestion with $\text{HNO}_3/\text{Br}_2/\text{HF}/\text{HCl}$. Dilute HCl was used to extract sulfate from the bulk solids; concentrations were determined by ICP-AES. Particle-size distribution was determined using a laser particle size analyzer (Malvern Mastersizer; ISO-13320, Panalytical, Almelo, The Netherlands). Specific gravity (GS) was measured using a gas pycnometer (Micromeritics Accupyc 1330, Micromeritics, Norcross, GA, USA).

The mineralogical compositions of the raw tailings samples were determined by X-ray diffraction (XRD) using a Bruker AXS Advance D8 (Bruker, Billerica, MA, USA) equipped with a copper anticathode, scanning over a diffraction angle (2θ) range from 5 to 60. Scan settings were 0.005° 2θ step size and 1 s counting time per step. The DiffracPlus EVA software (v. 9.0 rel. 2003) was used to identify mineral species. The TOPAS software (v. 2.1; Bruker, Billerica, MA, USA) was used to quantify the abundance of all identified mineral species implementing a Rietveld refinement. The absolute precision of this quantification method is ± 0.5 –1 wt % [41,42]. Before XRD analysis, samples were pulverized in isopropyl alcohol using a micronizing mill with corundum grinding media for 15 min to obtain ≈ 90 wt % $< 10 \mu\text{m}$.

Sample mineralogy was further investigated by optical and electronic microscopy observations. Polished sections of bulk samples as well as the flotation products were prepared using an epoxy resin for reflected light microscopy. Scanning electron microscope (SEM) observations on polished sections using backscattered electrons (BSE) were performed using a Hitachi S-3500N microscope (Silicon Drift Detector Bruker, Bruker, Billerica, MA, USA) equipped with an X-ray energy dispersive spectrometer (EDS; Silicon drift spectrometer X-Max 20 mm^2) operated by INCA software (450 Energy). The operating conditions were 20 keV, $\approx 100 \mu\text{A}$ and 15 mm working distance.

To explain the Au deportment, the pyrite and chalcopyrite minerals in both samples (sulfide concentrates and tailings) were analyzed using microprobe analyses (Electron Probe Micro-Analysis (EPMA), Cameca SX-100) [43]. An accelerating voltage of 15 kV, a beam current of 20 nA (counting time 15 s, background 0 s) were used for major elements (Fe, S, Cu, Co, Ni, Zn, and As) and 120 nA for Au (counting time 60 s, background 15 s) at the same resolution/beam size.

2.2.2. Static Tests

The most commonly used static tests to predict acid-generating potential is the acid–base accounting (ABA) test [44–46]. The ABA test measures the balance between the acid-generating potential (AP) and neutralizing-potential (NP) of a given sample. NP values were obtained using the Sobek method [47] as modified by Lawrence and Wang [45] and each NP measurement was performed in duplicate. AP was calculated using the sulfide sulfur fraction, which was obtained by subtracting the sulfate fraction from the total sulfur assay ($AP = 31.25 \times \% \text{ sulfur}$). Both AP and NP are expressed in kg CaCO_3/t . The net neutralization potential (NNP) was calculated by subtracting the AP value from the NP. NNP values $< -20 \text{ kg CaCO}_3/\text{t}$ indicate an acid-producing material, whereas materials with $NNP > 20 \text{ kg CaCO}_3/\text{t}$ are considered acid-consuming. An uncertainty zone exists between the range $20 > NNP > -20 \text{ kg CaCO}_3/\text{t}$ [48]. Another useful tool to evaluate AMD production potential is the NP to AP ratio. Typically, a material is considered non-acid generating if the $NP/AP > 2.5$, uncertain if $2.5 > NP/AP > 1$, and acid-generating if $NP/AP < 1$ [49].

2.2.3. Environmental Desulfurization by Froth Flotation

All flotation tests were carried out with a Denver D-12 lab flotation machine (2.5 L cell volume). All flotation tests were conducted on the southern tailings samples, which were generally characterized by high sulfur contents (Table 1). The pH during flotation was ~ 5 because the tailings' pore water was already acidic and the targeted solid percentage was around 30 solid wt % for all tests. The conditioning time was 3 min after the addition of a potassium amyl xanthate (PAX) collector (at various concentrations) and a frother (Methyl Isobutyl Carbinol (MIBC); $50 \mu\text{g}/\text{kg}$ of tailings). An activator of copper sulfate (CuSO_4) was used to reactivate the oxidized sulfide surfaces. The speed of the rotor-stator was adjusted to 1200 rpm with free airflow injection. To obtain consistent results, the same operator manually removed the froths with a spatula for all of the flotation tests. The pH was measured and adjusted by adding diluted NaOH solution to increase the pH. A summary of the flotation tests is presented in Table 1.

Table 1. Reagents used in the flotation tests.

Test Nbr	CuSO_4 (g/t)	KAX (g/t)	MIBC (g/t)
1	100	100	50
2	100	50	50
3	100	25	50
4	0	100	50
5	0	50	50
6	0	25	50

2.2.4. Kinetic Tests (Weathering Cells) Procedure

Representative samples of raw tailing (ST) and desulfurized tailings (DT), were selected for kinetic tests with weathering cells similar to the ones used by Cruz et al. [50]. The method uses a thin layer of sample and more frequent flushing–drying cycles compared to the ASTM D5744-96 humidity cell test [51]. The main advantage of this weathering cell test is its rapidity and the small volume of material required [52,53].

Approximately 67 g (dry weight) of tailings were placed in a 100 mm diameter Buchner funnel equipped with a glass-fiber filter. A seven-day cycle consisted of two days of exposure to ambient air, leaching on the third day, three days of exposure to air, and finally flushing during the seventh day. The flushes consisted of adding 50 mL of deionized water to the top of the Buchner funnel. The leachate was recovered by applying a slight suction on a filtering flask after 3 h of contact with the sample. The total duration of the experiments was 27 cycles (13 weeks).

The leachates recovered after each cycle were filtered using a $0.45 \mu\text{m}$ nylon filter and analyzed for several geochemical parameters to understand the tailings' reactivity, oxidation kinetics, metal

solubility, and the overall leaching behavior of the materials. For each sample, pH, Eh, electrical conductivity, metal concentrations, acidity, and alkalinity were analyzed. These data were compiled as instantaneous and cumulative loads, as well as elemental depletion curves that were based on the volume and composition of the leachates and the initial geochemistry of the solid samples. Filtered leachates were acidified with 2% HNO₃ to avoid metal precipitation. The resulting solutions were analyzed by ICP-AES to determine metal and sulfate concentrations.

3. Results

3.1. Sample Characterizations

The physical, chemical, and mineralogical properties of the different mine tailings are shown in Table 2. The specific gravity of all tailings samples was around 2.9 g/cm³. In terms of particle-size distribution, the Tiout mine tailings showed a silty characteristic, with a D₈₀ in the range of 100–230 µm. The NT and CT showed very low sulfur contents (0.4 and 0.06 wt %, respectively), while the ST contained up to 1.5 wt % sulfur. As the sulfur content was relatively low in the three samples related to low content of sulfide minerals, the high iron content (7.9–5 wt %) was related to the presence of iron-rich minerals such as hematite. Aluminum (~4–5 wt %), potassium (~2 wt %), manganese (~0.2 wt %), and sodium (~0.2 wt %) are related to silicate minerals. The low concentrations of Ca and Mg (~0.4 wt %) in the tailings suggest a negligible carbonate content. The Cu and Zn contents were around 0.1 wt %, while Pb and As concentrations were lower than 0.05 wt %. A fire assay of the selected samples from the Tiout mine site showed significant concentrations of precious metals, including 3–5 g/t of Au and 23–37 g/t of Ag.

Table 2. Physical, chemical and mineralogical composition of the Tiout tailings.

Characteristics	Northern Tailings (NT)	Central Tailings (CT)	South Tailings (ST)	Desulfurized Tailings (DT)	Sulfide Rich Tailings (SRT)
Physical properties					
SG (g/cm ³)	2.85	2.90	2.86	2.82	-
D ₈₀ (µm)	155	222	108	106	104
D ₅₀ (µm)	64	108	49	45	53
D ₁₀ (µm)	7	12	7	6	6
Chemical composition					
S _{total} (wt %)	0.37	0.061	1.5	0.51	21.57
S _{sulfate} (wt %)	0.08	0.055	0.17	0.38	0.64
S _{sulfide} (wt %)	0.29	0.006	1.33	0.13	20.93
Si (wt %)	38.24	37.68	34.12	33.6	18.7
Al (wt %)	4.31	5.19	4.26	4.89	4.04
Ca (wt %)	0.39	0.46	0.29	0.29	0.75
Fe (wt %)	8.29	8.54	7.95	8.52	22.52
K (wt %)	2	2.5	2	2.2	1.8
Mg (wt %)	0.42	0.464	0.369	0.44	0.61
Na (wt %)	0.1	0.22	0.21	0.22	0.63
Au (ppm)	5	3.95	3.36	-	-
Ag (ppm)	24	37	23	20	87
As (ppm)	300	190	846	860	860
Cu (ppm)	770	1140	924	870	2390
Pb (ppm)	290	110	296	280	740
Ti (ppm)	1190	1370	1680	1750	840
Zn (ppm)	1240	1130	1230	1140	3550
Mineralogical composition (%)					
Quartz SiO ₂	62.1	61.2	63.8	62.2	31.8
Muscovite KAl ₂ (Si ₃ Al)O ₁₀ (OH,F) ₂	19.2	18.5	16.2	20.1	15.2
Clinocllore (Mg,Fe) ₆ (Si,Al) ₄ O ₁₀ (OH) ₈	7.8	10.2	9.8	6.6	5.7
Hematite Fe ₂ O ₃	10.2	9.6	7.6	10.8	5.8
Pyrite FeS ₂	0.3	0.1	2.1	0.1	38.2
Sphalerite ZnS	0.2	0.2	0.2	0.1	0.6
Arsenopyrite FeAsS	0.1	0.1	0.2	0.2	0.2
Chalcopyrite CuFeS ₂	0.2	0.3	0.2	0.2	0.7
Galena PbS	0.1	0.0	0.0	0.0	0.8

The XRD results showed that the only sulfide detected in the ST was pyrite (1.7 wt %), which is in accordance with the S assays. Quartz was the most abundant mineral (73–77 wt %), with no carbonates detected (absence of neutralizing minerals) and low muscovite (5–10 wt %), clinocllore (4–5 wt %), and hematite (9–13 wt %) contents. Although analyzed, Cd, Co, Mo, Ni, and Ta were all below the detection limit of the ICP-AES and are not presented.

3.2. Flotation Test Results

Flotation experiments were carried out in order to select the optimal collector mix and to assess the effect of adding an activation reagent. As the ST had the highest sulfur content (in the form of sulfide minerals), these tailings were chosen for the desulfurization tests. Desulfurization was performed through sulfide bulk flotation tests. The sulfur recoveries obtained for various flotation test conditions are summarized in Figure 3.

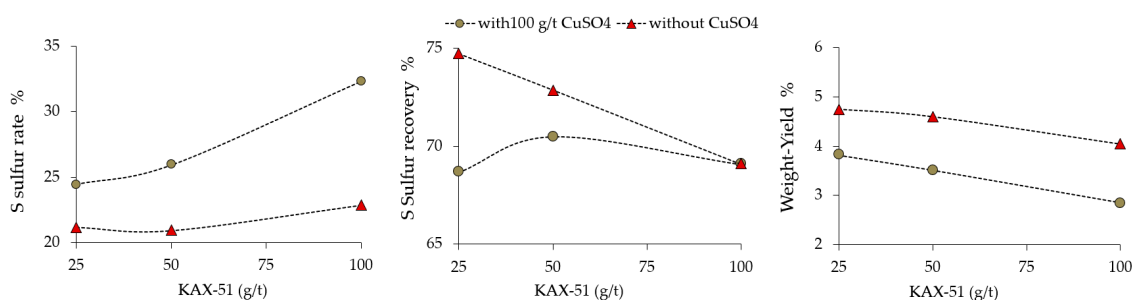


Figure 3. Yield weight and sulfur recovery during flotation tests (desulfurization).

The recovery yield of sulfur-bearing minerals was relatively high (68–74 wt %) with very negligible amounts of residual sulfides. Achieving a maximum recovery of around 73 wt % was possible with collector concentrations as low as 50 g/t and without any activators. Concentrate weight proportions were between 2.8% (for a collector concentration of 100 g/t and 100 g/t CuSO₄) and 4.7% (for a collector concentration of 25 g/t and without CuSO₄).

Results achieved using the optimal flotation conditions are presented in Figure 4. This experiment showed that the residual sulfur content in the tailings was <24% after 1 min and 13% after 10 min, which corresponds to a recovery of approximately 76% after 1 min and 87% after 10 min. The weight percentage of the concentrate was 2.9% after 1 min and 5.3% after 10 min.

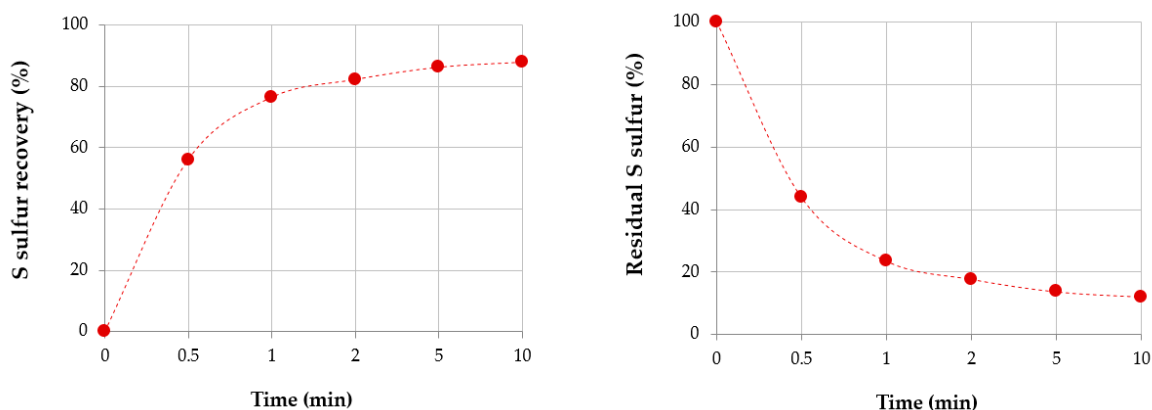


Figure 4. Flotation kinetic of the tailing: (a) % of S_{sulfide} recovery vs. time; (b) residual % S_{sulfur} vs. time.

The concentrate recovered from the first 30 s of the flotation test and from the desulfurized tailings were analyzed for their Au content. The results, which are displayed in Table 3, show that only around 4% of the initial gold in the ST sample was recovered and most of the gold remained within the desulfurized tailings, which could indicate unliberated gold within silicates.

Table 3. Au recovery within concentrate of flotation test.

Samples	Weight (g)	Au (g/t)	Au Distribution (%)
Initial sample (ST)	832	3.36	
Flotation concentrate	16.1	6.07	3.99
Flotation tailings	770.9	3.05	96.01

3.3. Mineralogy of Samples Obtained by Flotation Test and Gold Deportment

The sulfide concentrate sample contained mainly pyrite occurring in two different forms: (1) euhedral pyrite with flat faces and sharp edges (Figure 5a,c); and (2) anhedral pyrite represented by grains that show no well-formed crystal faces (xenomorphic) and grains overlapping one another (Figure 5a). Chalcopyrite, pyrrhotite, sphalerite, and galena were also present in trace amounts (Figure 5c,e). Chalcopyrite was often associated with pyrite as inclusions (Figure 5c).

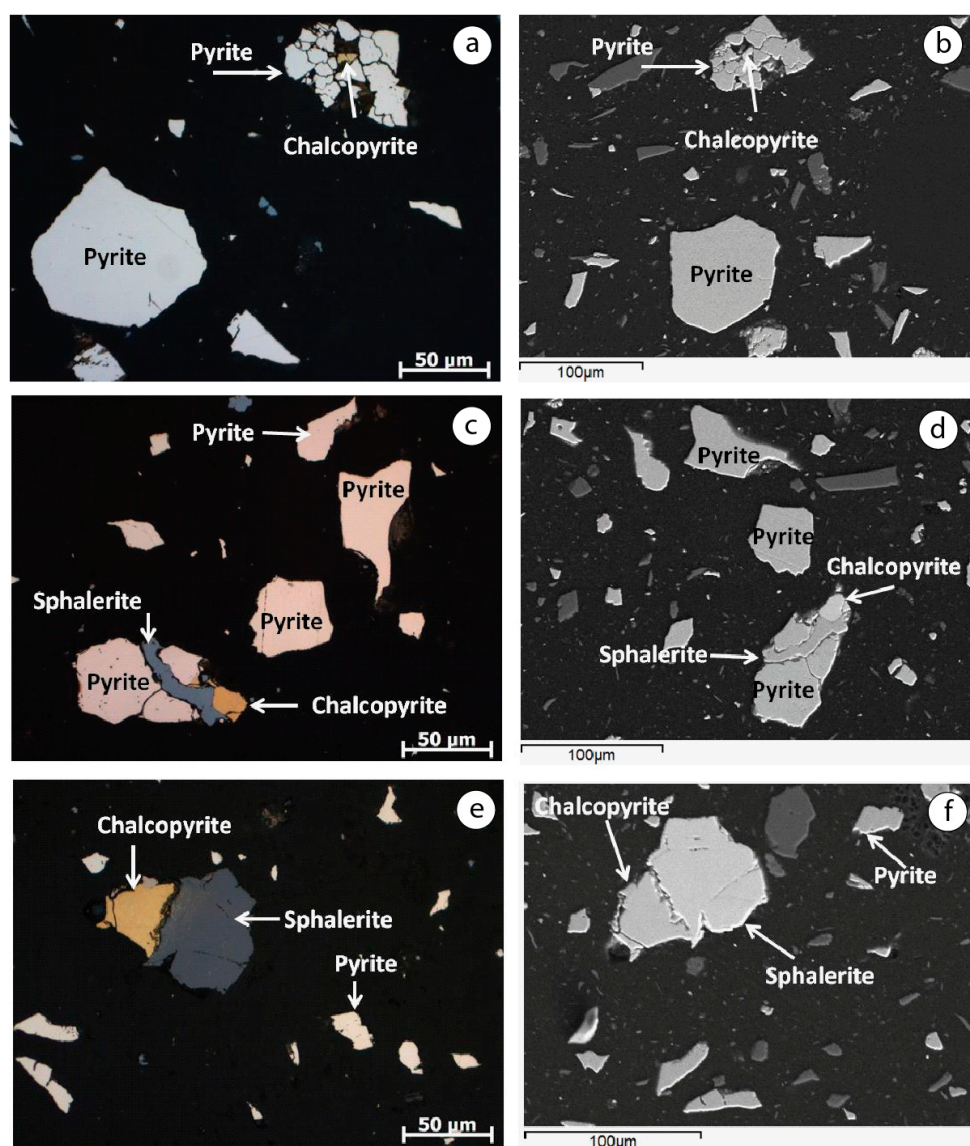


Figure 5. The identified sulfide minerals within the concentrate obtained from the flotation test; optical microscopy (a,c,e) and scanning electron microscopy (SEM) (b,d,f).

The tailings sample from the flotation test contained traces of chalcopyrite, sphalerite, pyrite and pyrrhotite with sizes generally lower than 20 μm . Chalcopyrite and pyrite were almost encapsulated

(Figure 6a,e) or attached to the gangue minerals (Figure 6c). The sample contained significant hematite and amorphous iron oxides as a result of pyrite oxidation (Figure 6g).

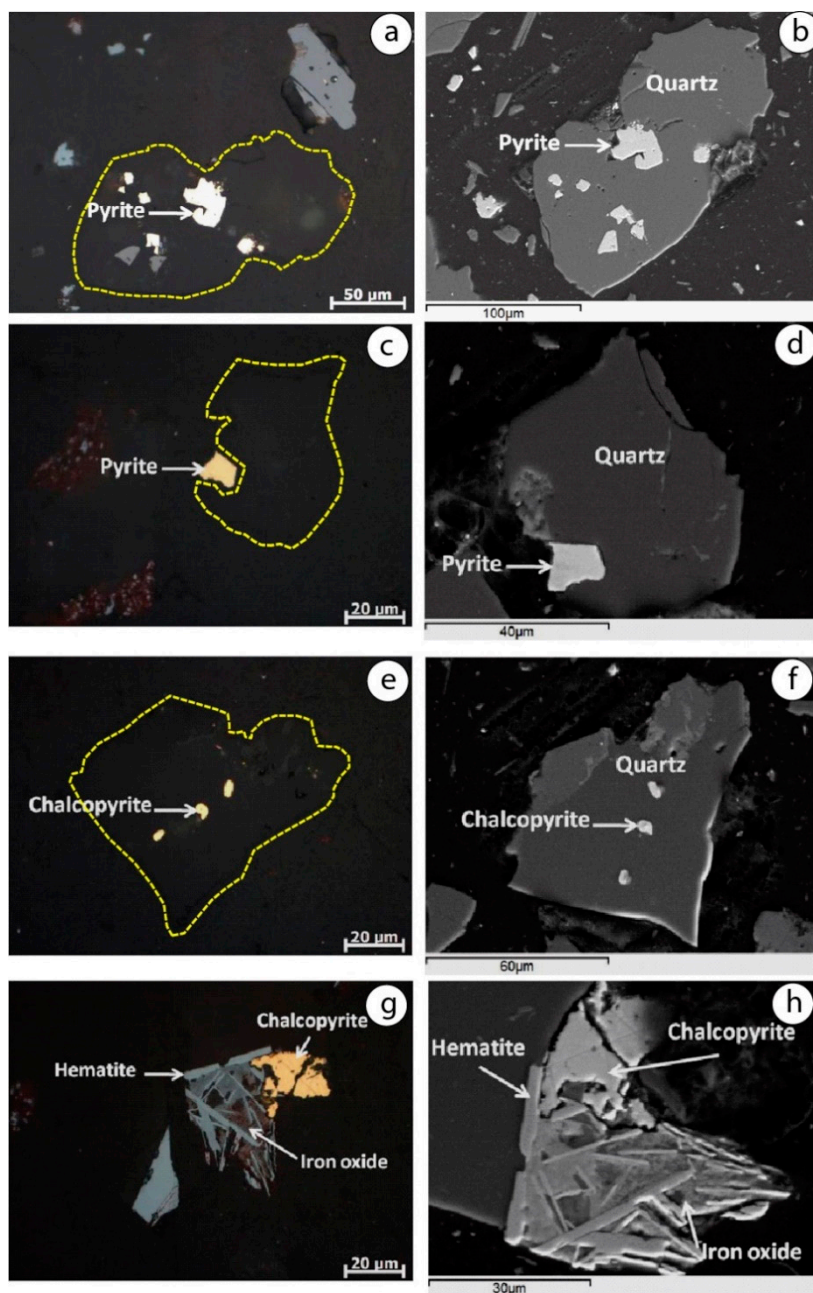


Figure 6. The identified sulfide minerals within the desulfurized tailings obtained from the flotation test; optical microscopy (a,c,e,g) and SEM (b,d,f,h).

Results from the EPMA (Table 4) show that 100% of Au in the concentrate was associated within the pyrite lattice. However, in the desulfurized tailings, only 0.4% of the total Au (3.05 g/t) was related to the pyrite. This could potentially be due to (1) insufficient statics in the EPMA measurements in the tailings; only 35 grains were analyzed instead of 104 in the concentrate, and/or (2) the presence of sub-micrometric gold locked in sulfides, iron-oxides, or gangue minerals (quartz) that the microscopic observations could not capture. Since the amount of the structural Au in the desulfurized sample was very low (0.4% of 3.05 g/t), and the sample contained substantial amounts of hematite and amorphous iron oxides resulting from pyrite oxidation, the Au was most probably associated with hematite

and Fe-oxides as sub-micrometric particles as already demonstrated by Benzaazoua et al. [43]. This suggests that, prior to weathering, the Au was refractory within the Tiouit ore body and explains its losses at such high amounts [38]. On the other hand, exploratory results from three independent laboratories showed up to 86% Au recovery from the Tiouit tailings can be attained by regrinding and cyanide-in-leach or cyanide-in-pulp processing, thus confirming the non-refractory behavior of Au.

Table 4. Compilation of the Electron Probe Micro-Analysis (EPMA) analyses of pyrite and chalcopyrite for the structural Au quantification.

Au Occurrence	Flotation Concentrate	Flotation Tailings
Total Au in the samples (by fire-assay, g/t)	6.07	3.05
Structural Au in Pyrite and chalcopyrite (g/t)	6.14	0.012
Structural Au in Pyrite (g/t)	6.04	0.01
Structural Au in Chalcopyrite (g/t)	0.06	0.002
% of structural Au compared to total Au	100%	0.4%

3.4. Static Test Prediction

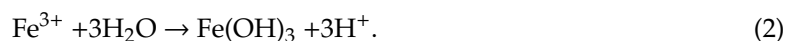
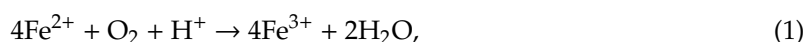
The ABA results, based on the Sobek et al. [47] test modified by Lawrence and Wang [45], are shown in Table 5. The Tiouit tailings showed a low NP (4–5 kg CaCO₃/t) and an AP of 0.1–9 kg CaCO₃/t. The ST showed the highest AP (41 kg CaCO₃/t) due to their high sulfide content (1.3 wt % S). According to the classification criteria proposed by Miller et al. [48], only the ST of Tiouit is potentially acid-generating. In contrast, the acid-generating potentials of the NT and CT are uncertain. Based on the NP/AP ratio [50], the ST and NT are acid-generating, while the CT is non-acid generating. Importantly, this acid-generating potential does not take into account the possible existence of Fe and sulfate secondary minerals that could contribute to the materials' acidities [54,55].

Table 5. Static test results of the Tiouit tailings.

Characteristics	Northern Tailings Pond (NT)	Central Tailings Pond (CT)	South Tailings Pond (ST)
AP (kg CaCO ₃ /t)	9.1	0.2	41.6
NP (kg CaCO ₃ /t)	5	5.4	4.2
NNP (kg CaCO ₃ /t)	−4	5.3	−37.4
NP/AP	0.6	29.0	0.1

3.5. Kinetic Test Results

For the initial tailings, the pH oscillated around 4 (2.8–5), and for the desulfurized tailings, the pH was slightly high and fluctuated around 5 (2.8–6.6) due to its low sulfide content after desulfurization ($S_{\text{sulfide}} = 0.13$ wt %). Both the initial and desulfurized tailings generated leachates with low pH values, however, this was only partially due to sulfide oxidation. Most likely the majority of the acid generation was related to the solubilization of secondary oxy-hydroxide minerals (Figure 6g). As the tailings were free of carbonates, they had no significant neutralizing potential. The solubilized Fe²⁺ might oxidize into Fe³⁺ under acidic conditions (Equation (1)), with subsequent hydrolysis generating acidity (Equation (2)). In addition to oxygen, acidity could also provide from the biological processes that could happen within these kind of conditions (*Acidithiobacillus*).



Eh values were slightly higher for the initial ST compared to the desulfurized tailings, indicating an oxidizing environment in agreement with their high sulfur content (152–296 mV and 91–251 mV,

respectively for initial tailing and desulfurized tailing samples) (Figure 7). For electrical conductivity (EC) and all dissolved elements, the measured values in the first nine recovered leachates showed the highest values compared to the subsequent rinsing cycles for both samples. The highest EC values (6270 $\mu\text{S}/\text{cm}$ for the two samples) and dissolved elements (SO_4^{2-} , Fe, Cu, Zn, Ca) were recorded at the beginning of the tests, presumably due to the dissolution of oxidation products generated by in situ weathering. In fact, EC and dissolved elements resulting from sulfide oxidation (SO_4^{2-} , Fe, Cu, Zn) and neutralization reactions (Ca, Mg) decreased and stabilized after the 9th cycle of the test, reaching a steady state (Figure 7). The EC and dissolved ions associated with oxidation/neutralization reactions were higher in the leachates recovered from the initial tailings sample than those of the desulfurized tailings (Figure 7), indicating the effectiveness of the desulfurization process at improving the environmental behavior of the tested mine tailings [56,57].

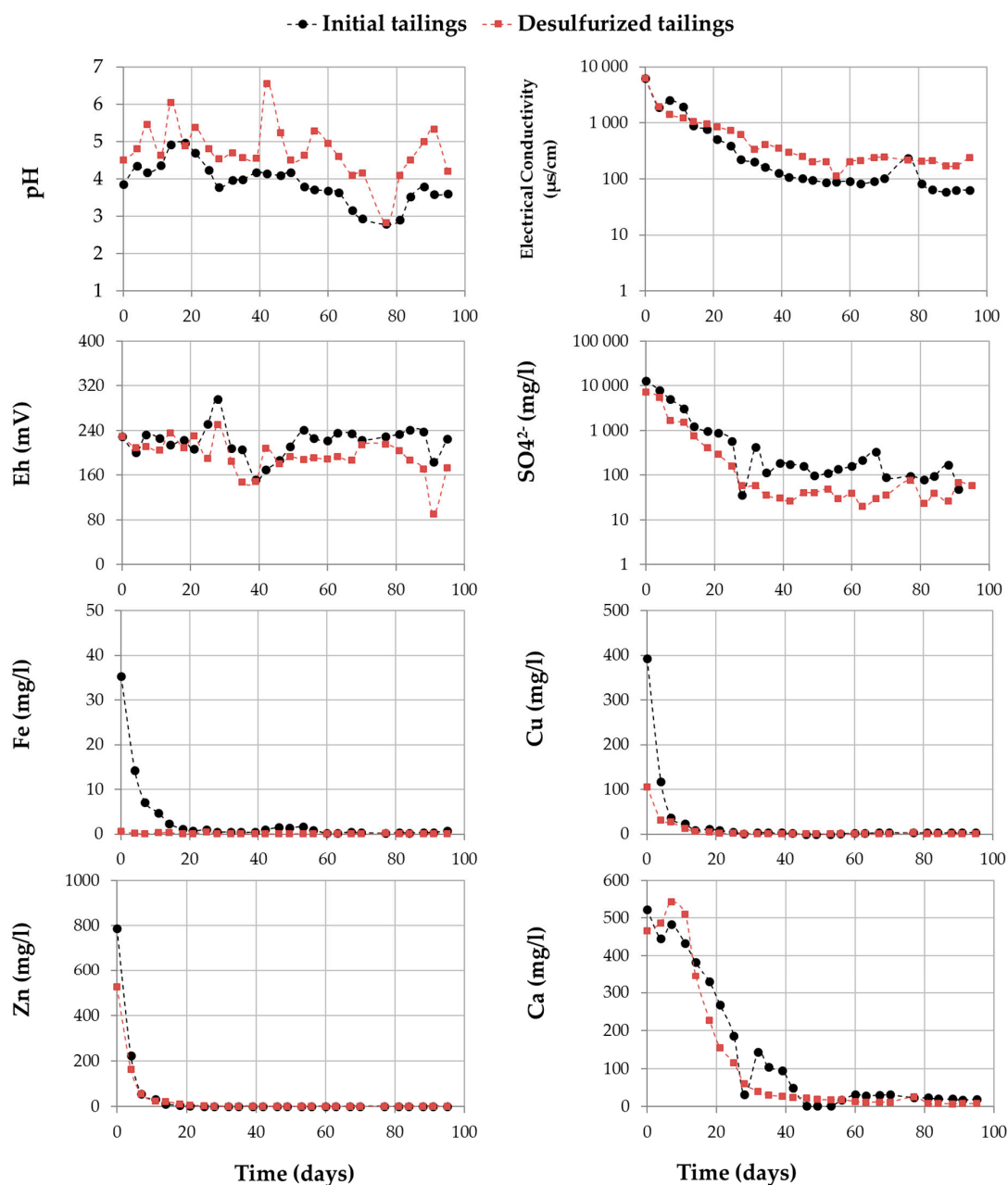


Figure 7. Evolution of pH, Eh, electrical conductivity (EC), and dissolved SO_4 , Fe, Cu, Zn, and Ca in leachates after 27 kinetic test cycles.

4. Conclusions

Approximately 743,000 tons of tailings were generated at the Tiouit mine between 1950 and 1996 and are now stored in three tailings ponds around the mine site. The tailings are characterized by low sulfur contents (0.06–1.3 wt %), with sulfur present mostly in pyrite, as well as in trace amounts of chalcopyrite. These tailings, which are acid-generating according to static tests, have been exposed to atmospheric weathering and erosion for 60 years with no reclamation strategy in place. The Tiouit tailings are, however, also a potential secondary resource due to the presence of Au (3.36–5 ppm) and Ag (24–37 ppm). The residual grades of Au and Ag were originally refractory (inserted within sulfides), but the transformation of sulfides to oxy-hydroxides (due to natural weathering) has allowed for their recovery. Desulfurization of the southern tailings was achieved through flotation as a technique for controlling the production of AMD. The acid-generating potential of the desulfurized sample was assessed by kinetic testing. Geochemical data showed that desulfurization allows for good but not completely effective sulfide recovery. Furthermore, the desulfurized tailings produced leachates with slightly higher pH values than the initial tailings and were less loaded in terms of sulfate and dissolved metals.

Gold recovery from the flotation concentrate sample was only 4%, which suggests that the Au is no longer associated with sulfides. The flotation results helped to determine an adequate amount of activator and collector (50 g/t) to achieve sulfide recovery with the lowest weight-yield. As the remaining sulfides are almost entirely encapsulated, they are likely unreactive and, therefore, there was no need for additional desulfurization. Meanwhile, it is important to confirm these results with other laboratory tests on other samples and at pilot scale during the possible reopening of the flotation plant. In a wider context, it is always important to characterize the polluting potential of tailings in closed mines as well as the potential value of any residual metals. This may allow economically feasible mine waste-processing strategies (already milled ore) to be implemented, instead of very costly mitigation/reclamation of mine sites.

Author Contributions: A.N. conducted the majority of the flotation tests aside from the physical and chemical characterizations. The mineralogical characterization was conducted by H.B. The interpretation of results and writing were done by A.N. and Y.T. under the supervision of M.B. and R.H.

Funding: This work was supported through the International Research Chairs Initiative, a program funded by the International Development Research Centre and supported by the Canadian Research Chairs program, Canada.

Acknowledgments: Our acknowledgements go to the International Development Research Centre for funding and to the Unité de Recherche et de Service en Technologie Minérale (UQAT) for their technical support.

Conflicts of Interest: The authors declare no conflict of interest.

Abbreviations

AP	Acid-generating potential
CT	Central tailings
EC	Electrical conductivity
Eh	Redox potential
DT	Desulfurized tailings
EDS	Energy dispersive spectroscopy
SG	Specific gravity
MIBC	Methyl Isobutyl Carbinol
NT	Northern tailings
NNP	Net neutralization potential
NP	Acid neutralizing potential
ST	South tailings
SEM	Scanning electron microscopy
XRD	X-ray diffraction

References

1. Simate, G.S.; Ndlovu, S. Acid mine drainage: Challenges and opportunities. *J. Environ. Chem. Eng.* **2014**, *2*, 1785–1803. [\[CrossRef\]](#)
2. Kefeni, K.K.; Msagati, T.A.; Mamba, B.B. Acid mine drainage: Prevention, treatment options, and resource recovery: A review. *J. Clean. Prod.* **2017**, *151*, 475–493. [\[CrossRef\]](#)
3. Neculita, C.-M.; Zagury, G.J.; Bussière, B. Passive treatment of acid mine drainage in bioreactors using sulfate-reducing bacteria. *J. Environ. Qual.* **2007**, *36*, 1–16. [\[CrossRef\]](#) [\[PubMed\]](#)
4. Bussière, B.; Aubertin, M.; Zagury, G.J.; Potvin, P.; Benzaazoua, M. Principaux défis et pistes de solution pour la restauration des aires d'entrepasage de rejets miniers abandonnées. In Proceedings of the Symposium 2005 sur l'environnement et les mines, Rouyn-Noranda, QC, Canada, 15–18 May 2005.
5. Aubertin, M.; Bernier, L.; Bussière, B. *Environnement et Gestion des Rejets Miniers [Ressource Électronique]: Manuel sur Cédérom*; Presses internationales Polytechnique: Mont-Royal, QC, Canada, 2002.
6. Parbhakar-Fox, A.; Lottermoser, B.G. A critical review of acid rock drainage prediction methods and practices. *Miner. Eng.* **2015**, *82*, 107–124. [\[CrossRef\]](#)
7. Hakkou, R.; Benzaazoua, M.; Bussière, B. Acid mine drainage at the abandoned Kettara mine (Morocco): 2. Mine waste geochemical behavior. *Mine Water Environ.* **2008**, *27*, 160–170. [\[CrossRef\]](#)
8. Ilankoon, I.M.S.K.; Tang, Y.; Ghorbani, Y.; Northey, S.; Yellishetty, M.; Deng, X.; McBride, D. The current state and future directions of percolation leaching in the Chinese mining industry: Challenges and opportunities. *Miner. Eng.* **2018**, *125*, 206–222. [\[CrossRef\]](#)
9. Parbhakar-Fox, A.; Lottermoser, B.; Bradshaw, D. Evaluating waste rock mineralogy and microtexture during kinetic testing for improved acid rock drainage prediction. *Miner. Eng.* **2013**, *52*, 111–124. [\[CrossRef\]](#)
10. Bouzahzah, H.; Benzaazoua, M.; Bussière, B.; Plante, B. Prediction of acid mine drainage: Importance of mineralogy and the test protocols for static and kinetic tests. *Mine Water Environ.* **2014**, *33*, 54–65. [\[CrossRef\]](#)
11. Hudson-Edwards, K. Tackling mine wastes. *Science* **2016**, *352*, 288–290. [\[CrossRef\]](#)
12. Ritcey, G.M. *Tailings Management: Problems and Solutions in the Mining Industry*; Elsevier Science Publishers: Amsterdam, The Netherlands, 1989.
13. Mackay, I.; Mendez, E.; Molina, I.; Videla, A.R.; Cilliers, J.J.; Brito-Parada, P.R. Dynamic froth stability of copper flotation tailings. *Miner. Eng.* **2018**, *124*, 103–107. [\[CrossRef\]](#)
14. Lutandula, M.S.; Maloba, B. Recovery of cobalt and copper through reprocessing of tailings from flotation of oxidised ores. *J. Environ. Chem. Eng.* **2013**, *1*, 1085–1090. [\[CrossRef\]](#)
15. Edraki, M.; Baumgartl, T.; Manlapig, E.; Bradshaw, D.; Franks, D.M.; Moran, C.J. Designing mine tailings for better environmental, social and economic outcomes: A review of alternative approaches. *J. Clean. Prod.* **2014**, *84*, 411–420. [\[CrossRef\]](#)
16. Falagán, C.; Grail, B.M.; Johnson, D.B. New approaches for extracting and recovering metals from mine tailings. *Miner. Eng.* **2017**, *106*, 71–78. [\[CrossRef\]](#)
17. Alcalde, J.; Kelm, U.; Vergara, D. Historical assessment of metal recovery potential from old mine tailings: A study case for porphyry copper tailings, Chile. *Miner. Eng.* **2018**, *127*, 334–338. [\[CrossRef\]](#)
18. Yin, Z.; Sun, W.; Hu, Y.; Zhang, C.; Guan, Q.; Wu, K. Evaluation of the possibility of copper recovery from tailings by flotation through bench-scale, commissioning, and industrial tests. *J. Clean. Prod.* **2018**, *171*, 1039–1048. [\[CrossRef\]](#)
19. Park, J.; Han, Y.; Lee, E.; Choi, U.; Yoo, K.; Song, Y.; Kim, H. Bioleaching of highly concentrated arsenic mine tailings by *Acidithiobacillus ferrooxidans*. *Sep. Purif. Technol.* **2014**, *133*, 291–296. [\[CrossRef\]](#)
20. Lee, E.; Han, Y.; Park, J.; Hong, J.; Silva, R.A.; Kim, S.; Kim, H. Bioleaching of arsenic from highly contaminated mine tailings using *Acidithiobacillus thiooxidans*. *J. Environ. Manag.* **2015**, *147*, 124–131. [\[CrossRef\]](#) [\[PubMed\]](#)
21. Borja, D.; Lee, E.; Silva, R.A.; Kim, H.; Park, J.H.; Kim, H. Column bioleaching of arsenic from mine tailings using a mixed acidophilic culture: A technical feasibility assessment. *J. Korean Inst. Resour. Recycl.* **2015**, *24*, 69–77.
22. Chen, T.; Lei, C.; Yan, B.; Xiao, X. Metal recovery from the copper sulfide tailing with leaching and fractional precipitation technology. *Hydrometallurgy* **2014**, *147*, 178–182. [\[CrossRef\]](#)
23. Golik, V.; Komashchenko, V.; Morkun, V. Innovative technologies of metal extraction from the ore processing mill tailings and their integrated use. *Metall. Min. Ind.* **2015**, *7*, 49–52.

24. Taha, Y.; Benzaazoua, M.; Mansori, M.; Yvon, J.; Kanari, N.; Hakkou, R. Manufacturing of ceramic products using calamine hydrometallurgical processing wastes. *J. Clean. Prod.* **2016**, *127*, 500–510. [[CrossRef](#)]
25. Kinnunen, P.; Ismailov, A.; Solismaa, S.; Sreenivasan, H.; Räisänen, M.-L.; Levänen, E.; Illikainen, M. Recycling mine tailings in chemically bonded ceramics—A review. *J. Clean. Prod.* **2018**, *174*, 634–649. [[CrossRef](#)]
26. Qi, C.; Fourie, A.; Chen, Q.; Zhang, Q. A strength prediction model using artificial intelligence for recycling waste tailings as cemented paste backfill. *J. Clean. Prod.* **2018**, *183*, 566–578. [[CrossRef](#)]
27. Loutou, M.; Misrar, W.; Koudad, M.; Mansori, M.; Grase, L.; Favotto, C.; Taha, Y.; Hakkou, R. Phosphate Mine Tailing Recycling in Membrane Filter Manufacturing: Microstructure and Filtration Suitability. *Minerals* **2019**, *9*, 318. [[CrossRef](#)]
28. Brend, L.G. *Mine Wastes, Characterization, Treatment and Environmental Impacts*; Springer: Berlin, Germany, 2007.
29. Leppinen, J.; Salonsaari, P.; Palosaari, V. Flotation in acid mine drainage control: Beneficiation of concentrate. *Can. Metall. Q.* **1997**, *36*, 225–230. [[CrossRef](#)]
30. Benzaazoua, M.; Bussière, B.; Kongolo, M.; McLaughlin, J.; Marion, P. Environmental desulphurization of four Canadian mine tailings using froth flotation. *Int. J. Miner. Process.* **2000**, *60*, 57–74. [[CrossRef](#)]
31. Benzaazoua, M.; Kongolo, M. Physico-chemical properties of tailing slurries during environmental desulphurization by froth flotation. *Int. J. Miner. Process.* **2003**, *69*, 221–234. [[CrossRef](#)]
32. Bois, D.; Poirier, P.; Benzaazoua, M.; Bussière, B.; Kongolo, M. A feasibility study on the use of desulphurized tailings to control acid mine drainage. *Cim Bull.* **2005**, *98*, 1.
33. Mermillod-Blondin, R. Influence des Propriétés Superficielles de la Pyrite et des Minéraux Sulfurés Associés sur la Rétention de Molécules Organiques Soufrées et Aminées: Application à la Désulfuration Environnementale. Ph.D. Thesis, Institut National Polytechnique de Lorraine, Nancy, France, et École Polytechnique de Montréal, Montreal, QC, Canada, 2005.
34. Demers, I.; Bussière, B.; Benzaazoua, M.; Mbonimpa, M.; Blier, A. Column test investigation on the performance of monolayer covers made of desulphurized tailings to prevent acid mine drainage. *Miner. Eng.* **2008**, *21*, 317–329. [[CrossRef](#)]
35. Hakkou, R.; Benzaazoua, M.; Bussière, B. Acid mine drainage at the abandoned Kettara mine (Morocco): 1. Environmental characterization. *Mine Water Environ.* **2008**, *27*, 145–159. [[CrossRef](#)]
36. Alansari, A.; Mouguina, E.; Maacha, L. 1.5-Le gisement de Tiouit à Au-Cu-Ag (Massif néoproterozoïque du J. Saghro). In *Les principales mines du Maroc*; Mouttaqi, A., Rjimati, E.C., Maacha, L., Michard, A., Soulaïmani, A., Ibouh, H., Eds.; Editions du Service géologique du Maroc: Rabat, Morocco, 2011; Volume 564, pp. 53–57.
37. Chaker, M. Géochimie et Metallogenie de la Mine d'or de Tiouit, Anti-Atlas Oriental, Sud du Maroc. Ph.D. Thesis, Université du Québec à Chicoutimi, Saguenay, QC, Canada, 1997.
38. Roche-Invest. *Oral Communication (Confidential Report)*; Roche-Invest: Basel, Switzerland, 2016.
39. Alansari, A. La Mine D'or de Tiouit: Un Exemple de Veines Aurifères Mésothermales, Associées à Une Granodiorite d'âge Protérozoïque Supérieur (Massif panafricain du Jbel Saghro, Anti-Atlas, Maroc). Ph.D. Thesis, University Cadi Ayyad, Marrakech, Morocco, 1997; p. 284.
40. Alansari, A.; Sagon, J.P. Le gisement d'or de Tiouit (Jbel Saghro, Anti-Atlas, Maroc), un système mésothermal polyphasé à sulfures-or et hématite-or dans une granodiorite potassique d'âge protérozoïque supérieur. *Chron. Rech. Min.* **1997**, *527*, 3–25.
41. Pirard, E. Modal analysis of mineralogical blends using optical image analysis versus X-ray diffraction and ICP. In Proceedings of the 9th International Congress for Applied Mineralogy (ICAM), Brisbane, Australia, 8–10 September 2008; p. 673679.
42. Raudsepp, M.; Pani, E. Application of Rietveld analysis to environmental mineralogy. *Environ. Asp. Mine Wastes* **2003**, *31*, 165–180.
43. Benzaazoua, M.; Marion, P.; Robaut, F.; Pinto, A. Gold-bearing arsenopyrite and pyrite in refractory ores: Analytical refinements and new understanding of gold mineralogy. *Mineral. Mag.* **2007**, *71*, 123–142. [[CrossRef](#)]
44. Lawrence, R. Prediction of the behavior of mining and processing wastes in the environment. In *Proc. Western Regional Symposium on Mining and Mineral Processing Wastes*; Doyle, F., Ed.; Society for Mining, Metallurgy, and Exploration, Inc.: Littleton, CO, USA, 1990.
45. Lawrence, R.W.; Wang, Y. Determination of neutralization potential in the prediction of acid rock drainage. In Proceedings of the Fourth International Conference on Acid Rock Drainage, Vancouver, BC, Canada, 31 May–6 June 1997; pp. 451–464.

46. Lawrence, R.W.; Marchant, P.M. *Acid Rock Drainage Prediction Manual*; MEND/NEDEM Report 1.16.1b; Canadian Centre for Mineral and Energy Technology: Ottawa, ON, Canada, 1991.
47. Sobek, A.A.; Schuller, W.; Freeman, J.; Smith, R. *Field and Laboratory Methods Applicable to Overburdens and Minesoils*; US Environmental Protection Agency: Cincinnati, OH, USA, 1978; Volume 45268, pp. 47–50.
48. Miller, S.; Jeffery, J.; Wong, J. Use and misuse of the acid base account for “AMD” prediction. In Proceedings of the 2nd International Conference on the Abatement of Acidic Drainage, Montréal, QC, Canada, 16–18 September 1991; pp. 16–18.
49. Adam, K.; Kourtis, A.; Gazea, B.; Kontopoulos, A. Evaluation of static tests used to predict the potential for acid drainage generation at sulphide mine sites. *Trans. Inst. Min. Metall. Sect. A Min. Ind.* **1997**, *106*, A1.
50. Cruz, R.; Bertrand, V.; Monroy, M.; González, I. Effect of sulfide impurities on the reactivity of pyrite and pyritic concentrates: A multi-tool approach. *Appl. Geochem.* **2001**, *16*, 803–819. [[CrossRef](#)]
51. Bouzahzah, H.; Benzaazoua, M.; Bussière, B. A modified protocol of the ASTM normalized humidity cell test as laboratory weathering method of concentrator tailings. In Proceedings of the International Mine Water and the Environment (IMWA), Mine Water and Innovative Thinking, Sydney, NS, Canada, 5–9 September 2010; pp. 15–18.
52. Bouzahzah, H.; Benzaazoua, M.; Bussière, B.; Plante, B. ASTM Normalized Humidity Cell Kinetic Test: Protocol Improvements for Optimal Sulfide Tailings Reactivity. *Mine Water Environ.* **2015**, *34*, 242–257. [[CrossRef](#)]
53. Villeneuve, M. *Évaluation du Comportement Géochimique à Long Terme de Rejets Miniers à Faible Potentiel de Génération D’acide à L’aide D’essais Cinétiques*; Université de Montréal—Ecole Polytechnique Montréal: Montreal, QC, Canada, 2004.
54. Elghali, A.; Benzaazoua, M.; Bussière, B.; Bouzahzah, H. Determination of the available acid-generating potential of waste rock, part II: Waste management involvement. *Appl. Geochem.* **2019**, *100*, 316–325. [[CrossRef](#)]
55. Elghali, A.; Benzaazoua, M.; Bussière, B.; Genty, T. Spatial Mapping of Acidity and Geochemical Properties of Oxidized Tailings within the Former Eagle/Telbel Mine Site. *Minerals* **2019**, *9*, 180. [[CrossRef](#)]
56. Benzaazoua, M.; Bouzahzah, H.; Taha, Y.; Kormos, L.; Kabombo, D.; Lessard, F.; Bussière, B.; Demers, I.; Kongolo, M. Integrated environmental management of pyrrhotite tailings at Raglan Mine: Part 1 challenges of desulphurization process and reactivity prediction. *J. Clean. Prod.* **2018**, *162*, 86–95. [[CrossRef](#)]
57. Elghali, A.; Benzaazoua, M.; Bouzahzah, H.; Bussière, B.; Villarraga-Gómez, H. Determination of the available acid-generating potential of waste rock, part I: Mineralogical approach. *Appl. Geochem.* **2018**, *99*, 31–41. [[CrossRef](#)]



© 2019 by the authors. Licensee MDPI, Basel, Switzerland. This article is an open access article distributed under the terms and conditions of the Creative Commons Attribution (CC BY) license (<http://creativecommons.org/licenses/by/4.0/>).